Available online at www.sciencedirect.com
ScienceDirect
Journal of Molecular Catalysis A: Chemical 261 (2007) 104–111
JOURNAL OF MOLECULAR CATALYSIS A: CHEMICAL
www.elsevier.com/locate/molcata

Effect of reduction temperature on a spray-dried iron-based catalyst for slurry Fischer–Tropsch synthesis

Qing-Lan Hao [a,b], Fu-Xia Liu [a], Hong Wang [a], Jie Chang [a], Cheng-Hua Zhang [a], Liang Bai [a,*], Hong-Wei Xiang [a], Yong-Wang Li [a], Fan Yi [c], Bin-Fu Xu [c]

[a] *State Key Laboratory of Coal Conversion, Institute of Coal Chemistry, Chinese Academy of Sciences, P.O. Box 165, Taiyuan 030001, PR China*
[b] *College of Material Science & Chemical Engineering, Tianjin University of Science & Technology, Tianjin, PR China*
[c] *Department of Physics of Wuhan University, Wuhan, PR China*

Received 18 January 2006; received in revised form 20 July 2006; accepted 20 July 2006
Available online 7 September 2006

Abstract

An industrial iron-based catalyst (100Fe/5Cu/6K/16SiO_2, by weight) was characterized after reduction at different temperatures and after Fischer–Tropsch synthesis (FTS) in a stirred tank slurry reactor (STSR). The BET surface area and pore volume of the catalyst decreases with increasing reduction temperature, and the contrary trend was found for pore size. The iron phase compositions of catalysts reduced with syngas were strongly dependent on pretreatment conditions employed. Pretreatment with syngas at lower temperature prevents iron catalyst activation. Carburization was intensified with the increase in reduction temperature. The formation of iron carbides in reduced catalyst was necessary for obtaining stable high FTS activity. The relationship between the amount of CO_2 in tail gas during activation and the Fe^{3+} (spm) content in the reduced catalyst was observed. The rapid carburization at high reduction temperature resulted in the formation of a superparamagnetic Fe^{3+} core and an iron carbide layer of the reduced catalyst. FTS activity decreased with the increase in the reduction temperature, but the stability distinctly improved. It was found that the working catalyst loss in the heavier waxy products resulted in higher deactivation rate of the catalyst reduced at lower temperature. With the increase in the reduction temperature, the product distribution shifted towards the lower molecular weight products.

Keywords: Fischer–Tropsch synthesis; Spray-dried iron catalyst; Reduction temperature; Slurry reactor; Mössbauer effect spectroscopy

1. Introduction

Before Fischer–Tropsch synthesis (FTS) reaction, the iron-based catalyst precursor must be subjected to activation treatment. The purpose is to bring the catalyst into an active form for FTS reaction. The conditions for the pretreatment of the iron-based catalyst used for slurry phase FTS have significant effects on its activity and selectivity [1–5]. It has been well documented that H_2, CO or syngas can be used as reductive agent during the pretreatment [1–3,6,7]. H_2 pretreatment of precipitated iron-based catalysts is reported to result in more stable catalysts, but their activity is very low [1,3]. Several researches proposed that pretreatment of precipitated iron-based catalyst with CO was preferred [1–3,8]. However, carbon monoxide pretreatment is not favorable on an industrial scale due to the high investment to purify CO. The development of pretreatment of precipitated iron-based catalysts with syngas that leads to active catalysts is more attractive, because syngas pretreatment could be performed with the same gas that is used in the FTS, eliminating the need for a pure hydrogen or carbon monoxide stream. Suitably employed pretreatment conditions with syngas of precipitated iron-based catalysts could achieve resemblanc to the activation with CO reduction [2].

Kölbel and Ralek [9] have proposed that the syngas pretreatment at higher temperature will result in "supercarbonization" and will prevent activation at lower temperature. However, no experimental data were reported. Luo and Davis [10] have suggested that CO conversion increased as syngas activation temperature increased from 230 to 270 °C, and that the FTS activity showed dependence on the activation pressure. Pressure, space velocity, and the syngas composition for reduction could cause great effects on the catalyst performance. Due to the multi-

* Corresponding author. Tel.: +86 351 4124899; fax: +86 351 4124899.
E-mail address: lbai@sxicc.ac.cn (L. Bai).

1381-1169/$ – see front matter © 2006 Published by Elsevier B.V.
doi:10.1016/j.molcata.2006.07.056

effects during catalyst reduction, complex phenomena have been observed on the relationship between reduction conditions and FTS performance for precipitated iron-based catalysts, leading to the difficulty in reaching a fundamental understanding on the reduction mechanism. The correlation between bulk phase compositions of reduced catalysts and their activity has not well been understood, either.

In general, the precipitated iron-based catalysts just after calcination consist dominantly of the Fe_2O_3 phase. The activation of an iron catalyst with syngas occurs in two steps: facile reduction of hematite (Fe_2O_3) to magnetite (Fe_3O_4) followed by slow reduction of Fe_3O_4 to iron carbides. Various carbides and oxides are known to coexist when the iron-based catalysts are subjected to activation with syngas. The phase compositions of the catalysts are strongly dependent on the activation procedure employed. Although exposure of the reduced catalysts to FTS conditions causes further change in iron phase compositions, the phase compositions of reduced catalysts directly impact the subsequent catalytic activity, stability and selectivity. To initialize the formation of these phases is an important aspect of FTS. So the pretreatment conditions appear to be crucial in determining the ultimate FTS activity of syngas activated catalyst.

This paper will discuss the effect of reduction temperature with syngas on the catalytic performance. Catalyst samples reduced at different temperatures were withdrawn from the slurry reactor and characterized by X-ray diffraction (XRD) and Mössbauer effect spectroscopy (MES). This study is aimed at providing a better understanding of the relationship among pretreatment, activity, selectivity, and the phase compositions of precipitated spray-dried iron catalysts used in a slurry phase FTS process.

2. Experimental

2.1. Catalyst preparation

A typical iron-based catalyst was prepared by a combination of continuous co-precipitation and spray-drying techniques. A solution containing $Fe(NO_3)_3$ (>99.9%; Tianjin Chemical Co., PR China), $Cu(NO_3)_2$ (>99.9%; Tianjin Chemical Co.), and silica gel (SiO_2, 30.0%; Qingdao Ocean Chemical Co.) with an $Fe/Cu/SiO_2$ weight ratio of 100/5/16 was introduced into a 20 l precipitation vessel containing deionized water at $80 \pm 1\,^{\circ}C$. A sodium carbonate solution (Tianjin Chemical Co.) was added simultaneously into this precipitation vessel to maintain the pH at a constant value of 9.0 ± 0.1, as measured with a pH meter (PHS-25; Shanghai Leici Co., PR China). After precipitation, the precipitate was filtered out and washed. A K_2CO_3 (>99.9%, Tianjin Chemical Co.) solution and deionized water in the amounts required to obtain the desired K/Fe weight ratio of 6/100 were added to the cake filtered out, and the mixture was then reslurried and spray-dried. The temperature for spray-drying was 250 °C at the inlet, and the pressure was 2.5 MPa. The spray-dried powder as prepared, which has good spherical shape and physical strength for the application to the FTS sluury reactor, was calcined in air at 320 °C for 5 h before use. The final obtained fresh catalyst composition was $100Fe/5Cu/6K/16SiO_2$ (mass weight).

2.2. Reactor system

The FTS tests were carried out in a 1 dm^3 stirred tank slurry reactor (STSR) equipped with a sintered metal filter to allow the removal of wax products from the reaction system. Detailed description of the reactor has been provided elsewhere [11]. About 20 g of a fresh catalyst was loaded into the reactor and suspended in 320 g liquid paraffin (A.C, boiling point >340 °C). The syngas ($H_2/CO = 0.67$), derived from the mixture of pure H_2 (>99.95%) and pure CO (>99.99%), passed through a series of columns for removing tiny amounts of oxygen, sulfur, carbonyls and water before entering the reactor. The flow rates of the feed gases were controlled by using two Brooks 5850E mass flow meters. The syngas was preheated, and then was fed to the bottom of the reactor. The stirring speed for the impeller was maintained at 800 rpm.

H_2, CO, CH_4 and C_1–C_8 hydrocarbons (*n*-paraffins, *n*-olefins, and branched isomers) in tail gas were analyzed by an Agilent 6890N (HP) gas chromatograph (GC) with a 5 A molecular sieve column (Ar carrier) and an Al_2O_3 column (N_2 carrier) equipped with a TCD and a FID. Gas components were determined by the methane concentration correlation method. CO_2 in tail gas was measured periodically on-line using an Agilent 4890D GC (HP) equipped with a TCD (H_2 carrier) and quantified by the external standard method. The heavy wax and the oil products were analyzed using an Agilent 6890N (HP) GC with UA^+-(HT) stainless steel capillary column (FID, N_2 carrier) and an Agilent 6890N (HP) GC with DB-1 quartz capillary column (FID, N_2 carrier), respectively. Oxygenates in water products were measured by an Agilent 6890N (HP) GC with DB-WAX quartz capillary column (FID, N_2 carrier).

2.3. Reduction and reaction conditions

All activations were conducted in situ, using syngas ($H_2/CO = 0.67$) at 0.4 MPa, 1.0 NL/g-cat h and different temperatures. The catalyst slurry was heated from room temperature to 120 °C at a heating rate of 0.83 °C/min in flowing syngas and held at this temperature for 3 h. The reactor was then heated from 120 °C to different activation temperatures at a heating rate of 0.17 °C/min in the same flowing syngas and kept at desired temperature for 13 h. The detailed pretreatment conditions are summarized in Table 1. At the end of the pretreatment, the slurry

Table 1
Pretreatment conditions of the catalyst

Run no.	*T* (°C)	Reductant (H_2/CO)	Duration (h)	*P* (MPa)	GHSV (NL/g-cat h)
T240	240	0.67	13	0.4	1.0
T250	250	0.67	13	0.4	1.0
T260	260	0.67	13	0.4	1.0
T270	270	0.67	13	0.4	1.0
T280	280	0.67	13	0.4	1.0

was cooled down (or heated) to reaction temperature (250 °C) and the reactor was pressurized to operating pressure (1.5 MPa). After reaching the desired reaction temperature and pressure, the space velocity of syngas ($H_2/CO = 0.67$) was increased to 2 NL/g-cat h for FTS reaction tests.

2.4. Catalyst sample handling

During reduction and reaction tests, part of the catalyst suspended in the liquid paraffin was withdrawn from the reactor through a dip tube connected to a sampling trap. In order to prevent the exposure of the catalyst to oxidizing atmosphere, the sampling system was purged with argon prior to slurry withdrawal. The slurry samples from the sampling trap were treated to separate the catalyst from the heavy waxy products. After the extraction, the catalysts were sealed and stored in a glass holder immersed in ethanol to prevent exposure of the catalysts to air.

2.5. Catalyst characterization

The BET surface area, pore volume and the pore size distribution of the catalyst were determined by N_2 physisorption at 77 K using a Micromeritics ASAP 2500 instrument. The samples were degassed at 150 °C for 12 h before BET measurement.

The composition of the catalyst was determined by atomic absorption spectroscopy (AAS) on a TJA AtomScan16 absorption spectro-photometer.

XRD patterns of the catalyst samples were carried out on a D/max-RA X-ray diffractometer (Rigaku, Japan) equipped with a Cu Kα radiation. Standard powder XRD cards compiled by the Joint Committee on Powder Diffraction Standards (JCPDS) and published by the International Center for Diffraction Data were used to identify the iron phase presenting in the catalyst during reduction and reaction.

MES was measured with a Canberra series 40MCA constant-acceleration Mössbauer spectrometer (Canberra, USA) at room temperature. The radioactive source comprised 25 mCi of ^{57}Co in a Pd matrix. All spectra were analyzed with a set of independent Lorentzian lines and with the help of a non-linear least squares fitting procedure. The number of center channels and the increment of velocity per channel were determined by a standard α-Fe sample at room temperature. The hyperfine parameters, the isomer shift (IS), the quadruple splitting (QS), and the magnetic hyperfine field (Hhf) were used to identify the spectral components. Isomer shifts were reported with respect to α-Fe sample (99.99%, Alfa Aesar). Usually it was assumed that the Mössbauer area ratios are equal to the relative amount of the associated species.

3. Results and discussion

3.1. The catalyst reduction

In the reduction process conducted in syngas atmosphere, α-Fe_2O_3 is transformed rapidly to Fe_3O_4 and then slowly to Fe_xC. Correspondingly, the CO_2 content in tail gas during reduction process is measured periodically on-line using GC. It was suggested that the performance of CO_2 released during activation with syngas can be an indicator for the formation of the iron phases. Fig. 1 represents the change of the CO_2 content during the reduction process under different temperatures. The CO_2 content in tail gas rises monotonously to 7.31% and no maximum is observed at 240 °C. However, when the reduction temperature is increased above 250 °C, the CO_2 concentration in tail gas initial increases with extending reduction duration and passes through a maximum, afterwards gradually decreasing to stablized values. The maximum of CO_2 in tail gas during reduction increases with the increase in temperature. The CO_2 content increases rapidly to a maximum, suggesting that the reduction of α-Fe_2O_3 to Fe_3O_4. When the CO_2 concentration in tail gas is stabilized, the distinct iron phases are formed under the reduction conditions. No maximum of the amount of CO_2 in tail gas at 240 °C indicates that the reduction of catalyst is not completely, α-Fe_2O_3 phase being present in the reduced catalyst.

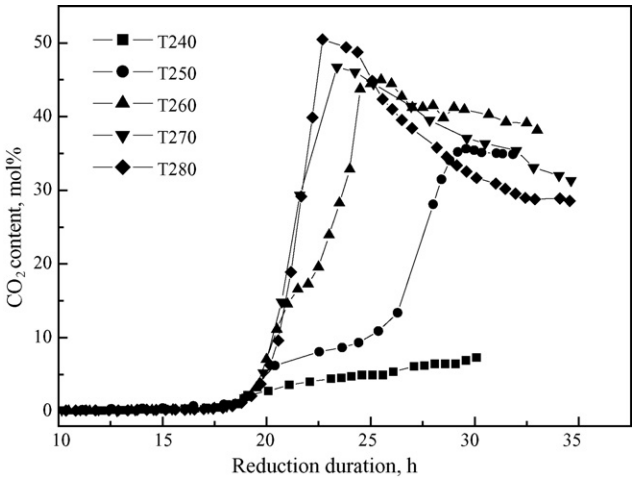

Fig. 1. The change of CO_2 content during the reduction process. Reduction conditions: 240–280 °C, 0.4 MPa, $H_2/CO = 0.67$, 1.0 NL/g-cat h.

3.2. Catalyst characterization

The textural properties of fresh and reduced catalysts are listed in Table 2. The BET surface area, pore volume and average pore size of the fresh catalyst are 94 m^2/g, 0.33 cm^3/g and 14 nm, respectively. The catalyst undergoes a volumetric change due to the iron phase transformation from the initial α-Fe_2O_3 to Fe_3O_4 and then to iron carbides during reduction. From Table 2, it can be seen that both BET surface area and pore volume of reduced catalysts decrease with the increase in reduction temperature, and the reverse trend is found for pore size. Decrease in the BET surface area and pore volume, and increase in average pore

Table 2
Textural properties of fresh and reduced catalysts

Catalysts	Fresh	T240	T250	T260	T270	T280
BET surface area (m^2/g)	94.32	62.47	59.81	57.47	55.82	54.10
Pore volume (cm^3/g)	0.33	0.29	0.27	0.26	0.28	0.24
Average pore size (nm)	14.14	24.79	25.70	25.75	25.92	28.22

Reduction conditions: 0.4 MPa, $H_2/CO = 0.67$, 1.0 NL/g-cat h.

size can be attributed to the partial collapse of the porous iron oxide/hydroxide framework [12], carbonaceous deposits [13] and the catalyst particles agglomeration during the pretreatment [14].

Bulk compositions in the fresh catalyst and samples after the pretreatment and reaction under the baseline conditions (250 °C, 1.5 MPa and 2.0 NL/g-cat h) are determined by XRD and MES. Although XRD has a better spatial resolution (>3–5 nm), it is difficult to make quantitative assignments due to the overlap of carbide peaks. So, MES is used as an effective method for providing quantitative information on the amount of various iron phases present in the catalyst samples [15]. The XRD patterns and MES spectra of fresh and reduced catalysts are shown in Figs. 2 and 3, respectively. Corresponding parameters of catalyst samples are summarized in Table 3.

The obtained XRD patterns have been plotted for 2θ values ranging from 25° to 75° since the most intensive peak of α-Fe_2O_3, Fe_3O_4 as well as the iron carbide phases fall within this range. XRD results indicate that Fe_2O_3 is the sole iron phase present in the fresh catalyst, which has characteristic peaks at 2θ values of 33.4°, 35.8°, 40.8°, 49.5°, 54.1°, 62.5° and 64.0°. MES spectra of the fresh catalyst include a sextet and a doublet. The sextet assigned to Fe_2O_3 of large crystallites shows a content of 32.9%, and the doublet typical of the superparamagnetic (spm) Fe^{3+} shows a content of 67.1%. It has been reported that the critical particle diameter for superparamagnetic in α-Fe_2O_3 is below 13.5 nm [16]. The presence of large amount of Fe^{3+} (spm) indicates that iron crystallites in the fresh catalyst is stabilized and dispersed by the addition of binder SiO_2.

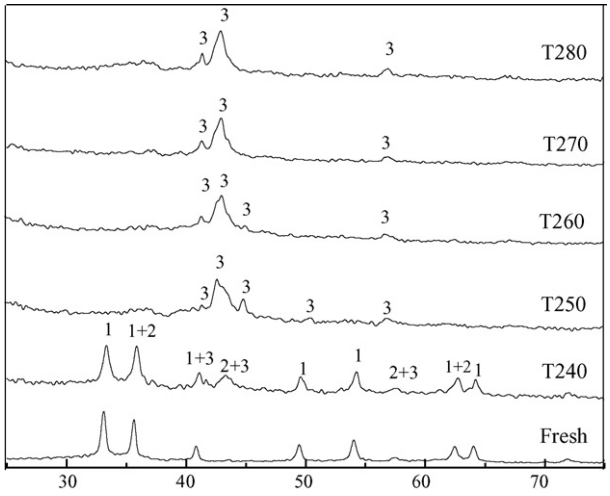

Fig. 2. XRD patterns of fresh and reduced catalysts. (1) Fe_2O_3, (2) Fe_3O_4 and (3) Fe_xC. Reduction conditions: 0.4 MPa, $H_2/CO = 0.67$, 1.0 NL/g-cat h.

As determined by XRD, the catalyst sample of test T240 is a mixture of Fe_2O_3, Fe_3O_4 and iron carbides. The iron phases of catalysts reduced at 250 °C and above are mainly mixtures of various iron carbides. XRD could only demonstrate the exis-

Table 3
Iron phases identified by XRD and MES in fresh and reduced catalysts

Run no.	Phases identified by XRD	Phases identified by MES	MES parameters			Area (%)
			IS (mm/S)	QS (mm/s)	Hhf (kOe)	
Fresh catalyst	α-Fe_2O_3	α-Fe_2O_3	0.40	−0.15	491	32.9
		Fe^{3+} (spm)	0.36	0.69	–	67.1
T240	Fe_xC, Fe_2O_3, Fe_3O_4	χ-Fe_5C_2	0.35	0.08	216	11.2
		ε′-$Fe_{2.2}C$	0.21	0.23	171	6.8
		Fe_3O_4 (A)	0.35	–	490	20.3
		Fe_3O_4 (B)	0.65	–	440	11.5
		α-Fe_2O_3	0.40	−0.20	518	3.3
		Fe^{2+} (spm)	0.96	1.88	–	21.6
		Fe^{3+} (spm)	0.36	0.78	–	25.3
T250	Fe_xC	χ-Fe_5C_2	0.40	−0.08	218.	24.5
		ε′-$Fe_{2.2}C$	0.23	0.14	174	38.7
		Fe^{2+} (spm)	0.99	1.83	–	26.6
		Fe^{3+} (spm)	0.35	0.91	–	10.2
T260	Fe_xC	χ-Fe_5C2	0.36	−0.03	219	21.1
		ε′-$Fe_{2.2}C$	0.25	0.08	172	44.5
		Fe^{2+} (spm)	0.94	1.75	–	23.1
		Fe^{3+} (spm)	0.24	0.91	–	11.3
T270	Fe_xC	χ-Fe_5C_2	0.29	0.10	233	17.3
		ε′-$Fe_{2.2}C$	0.24	0.09	172	49.4
		Fe^{2+} (spm)	0.60	1.5	–	20.6
		Fe^{3+} (spm)	0.32	0.89	–	12.7
T280	Fe_xC	χ-Fe_5C_2	0.36	−0.05	220	14.7
		ε′-$Fe_{2.2}C$	0.24	0.11	170	53.1
		Fe^{2+} (spm)	1.05	2.24	–	19.2
		Fe^{3+} (spm)	0.27	0.83	–	13.0

spm: superparamagnetic phase; reduction conditions: 0.4 MPa, $H_2/CO = 0.67$, 1.0 NL/g-cat h.

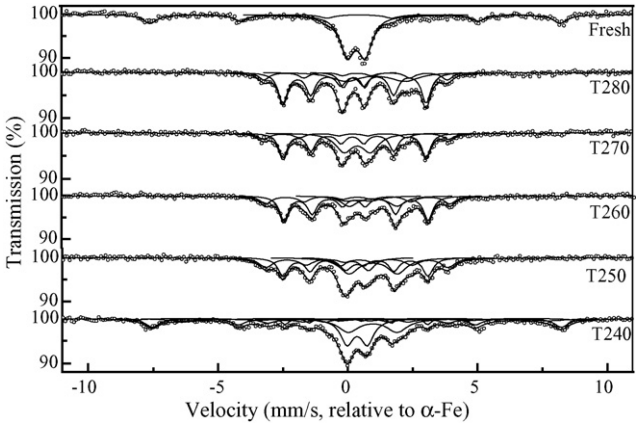

Fig. 3. Mössbauer spectra of fresh and reduced catalysts. Reduction conditions: 0.4 MPa, $H_2/CO = 0.67$, 1.0 NL/g-cat h.

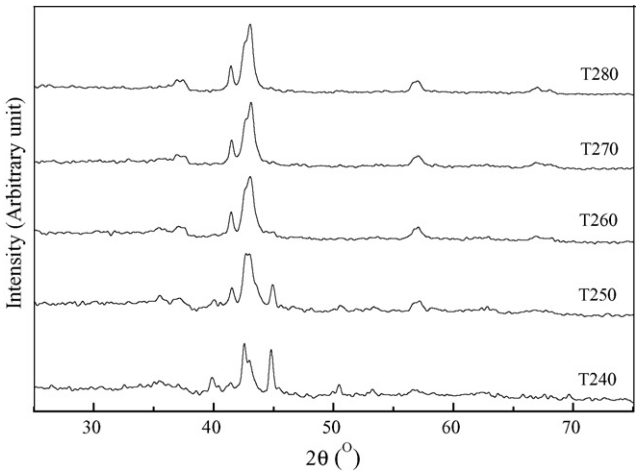

Fig. 4. XRD patterns of the used catalysts. Reaction conditions: 250 °C, 1.5 MPa, $H_2/CO = 0.67$, 2.0 NL/g-cat h.

tence of these iron carbides without distinguishing their type because of resolution limitation. As shown in MES measurements, the catalyst reduced at 240 °C comprises 31.8% Fe_3O_4, 21.6% Fe^{2+}(spm), 25.3% Fe^{3+}(spm), 11.2% χ-Fe_5C_2, 6.8% ε'-$Fe_{2.2}C$ and 3.3% Fe_2O_3. When the reduction temperature is increased, Fe_2O_3 and Fe_3O_4 phases of the reduced catalyst disappear; the phases are in a mixture state of ε'-$Fe_{2.2}C$, χ-Fe_5C_2, Fe^{2+} (spm) and Fe^{3+} (spm). The amount of carbides increases with the increase in reduction temperature. However, χ-Fe_5C_2 decreases with the increase in reduction temperature, and the reverse tendency is observed for ε'-$Fe_{2.2}C$. The results of XRD and MES clearly demonstrate that the iron phase compositions of reduced catalysts are strongly dependent on pretreatment conditions employed. According to the general understanding of active phases in iron based FTS catalysts, the pretreatment with syngas at higher temperature could improve the activity. This deduction is confirmed in subsequent reaction experiments.

When the reduction temperature increases above 250 °C, the amount of Fe^{3+} (spm) and carbides increases with increasing temperature, and the reverse trend is found for Fe^{2+} (spm). The content of Fe^{2+} (spm) in the reduced catalysts is higher than that of Fe^{3+} (spm). The carburization is enhanced at high reduction temperatures. The rapid carburization might results in the formation of a Fe^{3+} (spm) core and an iron carbides layer. The phenomena of a core of Fe_3O_4 surrounded by a surface layer of iron carbides were reported previously [17,18]. On the other hand, the amount of CO_2 released during activation and the content of Fe^{3+} (spm) in the reduced catalyst increase with the increases in reduction temperature. The possible reason is that CO_2 in tail gas is high enough to make the Fe^{3+} (spm) the stable phase compared to Fe^{2+} (spm) during activation.

Exposure of the reduced catalysts to FTS conditions causes further changes in iron phase compositions. The XRD patterns and MES spectra of used catalysts are shown in Figs. 4 and 5, respectively. XRD results and the MES parameters of used catalysts are summarized in Table 4. The iron phases of the used catalysts are identified as carbides by XRD, and are identified as χ-Fe_5C_2, ε'-$Fe_{2.2}C$ and Fe^{2+}/Fe^{3+} (spm) by MES. The total amount of carbides of the used catalyst is slightly smaller than that of the reduced catalyst. That is, the content of ε'-$Fe_{2.2}C$ and Fe^{3+} (spm) increases, while the amount of χ-Fe_5C_2 and Fe^{2+} (spm) decreases after FTS. The most reasonable explanation is that χ-Fe_5C_2 is further transformed to ε'-$Fe_{2.2}C$ during FTS. The decrease in the amount of carbides and Fe^{2+} (spm) is attributed to oxidation by high H_2O/H_2 and CO_2/CO ratios during FTS [3,18].

3.3. Activity and stability

To systematically investigate the effect of reduction temperature on FTS activity, stability, and selectivity, a series of FTS tests under the same reaction conditions are carried out. It is found that during the FTS the catalysts reduced under different temperatures exhibit significant differences in activity, stability and selectivity. The FTS activity measured by carbon monoxide conversion is shown in Fig. 6 and Table 5, and the catalyst deactivation rates (according to the molar percent of CO conversion decrease) are listed in Table 6. The initial activity decreases with the increase in the reduction temperature, from 76.4% (T240) to 58.4% (T280). The stability is improved with the increase in the reduction temperature. The deactivation rate decreases from 2.57%/d in run T240 to 0.33%/d in runs T270 and T280.

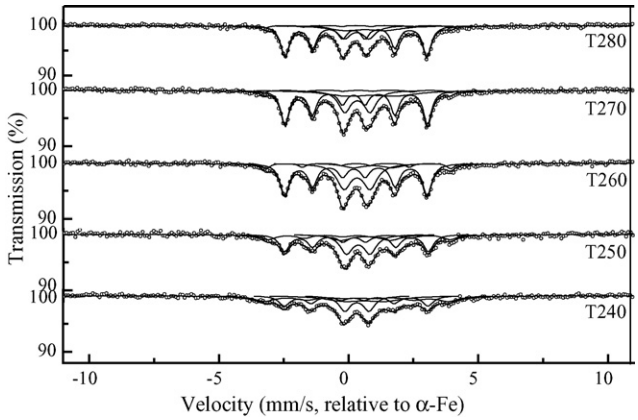

Fig. 5. Mössbauer spectra of used catalysts. Reaction conditions: 250 °C, 1.5 MPa, $H_2/CO = 0.67$, 2.0 NL/g-cat h.

Table 4
Iron phases identified by XRD and MES in used catalysts

Run no.	TOS (h)	Phases identified by XRD	Phases identified by MES	MES parameters			Area (%)
				IS (mm/s)	QS (mm/s)	Hhf (kOe)	
T240	473	Fe_xC	χ-Fe_5C_2	0.37	−0.16	222	29.1
			ε'-$Fe_{2.2}C$	0.22	0.14	172	28.1
			Fe^{2+} (spm)	0.61	1.58	–	20.0
			Fe^{3+} (spm)	0.32	0.94	–	22.8
T250	501	Fe_xC	χ-Fe_5C_2	0.35	0.08	218	17.9
			ε'-$Fe_{2.2}C$	0.24	0.19	173	40.9
			Fe^{2+} (spm)	0.64	1.90	–	14.2
			Fe^{3+} (spm)	0.36	0.91	–	27.0
T260	521	Fe_xC	χ-Fe_5C_2	0.33	0.10	221	7.8
			ε'-$Fe_{2.2}C$	0.25	0.08	171	53.8
			Fe^{2+} (spm)	0.94	1.50	–	7.8
			Fe^{3+} (spm)	0.33	0.10	–	30.6
T270	498	Fe_xC	χ-Fe_5C_2	0.34	−0.04	224	5.8
			ε'-$Fe_{2.2}C$	0.25	0.10	171	52.9
			Fe^{2+} (spm)	0.88	1.89	–	17.7
			Fe^{3+} (spm)	0.34	0.98	–	23.6
T280	501	Fe_xC	χ-Fe_5C_2	0.34	0.04	222	4.2
			ε'-$Fe_{2.2}C$	0.24	0.09	170	61.4
			Fe^{2+} (spm)	0.64	1.59	–	16.4
			Fe^{3+} (spm)	0.32	0.95	–	18.0

spm: superparamagnetic phase; reaction conditions: 250 °C, 1.5 MPa, $H_2/CO = 0.67$, 2.0 NL/g-cat h.

The highest initial activity is obtained in run T240. However, this high activity level cannot be maintained. Its stability is very poor, and the catalyst shows the highest deactivation rate. XRD and MES results show that the catalyst for the T240 test is not completely reduced. The amount of carbides in the bulk composition is smaller than those of others; Fe_2O_3 and Fe_3O_4 phases exist in the incompletely reduced catalyst. The incompletely reduced catalyst results in rapid reduction and carburization by exposure to FTS reaction conditions, which causes the highest initial and maximum CO conversion. With increasing reduction temperature to above 250 °C the amount of carbides increases while the conversion decreases. Rao et al. [2] reported that the catalyst undergoes changes in chemical composition while both the catalyst activity and selectivity remain essentially constant. The activity decreases because of the decrease in the BET surface area with increasing reduction temperature. At high reduction temperature the carbon deposition is relatively severe and the surface carbides of the reduced catalyst might be covered and blocked with inactive carbon species. The results suggest that the presence of some fraction of iron carbides is necessary for an iron catalyst to exhibit stable high activity. But the catalyst activity cannot be predicted solely from the bulk iron that is present as the carbides. The iron phase equilibrium and a layer of surface carbide may be responsible for high FTS activity. At the same, the catalyst attrition resistance played an important role in determining stable high activity. Increasing reduction temperature can efficiently prevent the working catalyst loss (see Fig. 7).

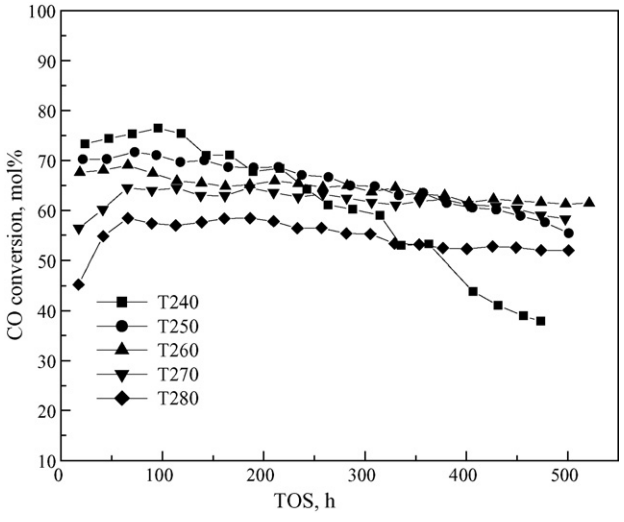

Fig. 6. Effect of reduction temperature on catalyst activities. Reaction conditions: 250 °C, 1.5 MPa, $H_2/CO = 0.67$, 2.0 NL/g-cat h.

XRD and MES results suggest that the carburization further occurs during FTS, meanwhile the reoxidation is also observed. χ-Fe_5C_2 phase in reduced catalysts is lowered at the end of FTS reaction, and the reverse tendency is found for ε'-$Fe_{2.2}C$ phase. The transformation from χ-Fe_5C_2 to ε'-$Fe_{2.2}C$, the reoxidation and inactive carbon deposition are the causes for slow deactivation of iron catalysts reduced at higher temperature. But the deactivation rate of the reduced catalyst at 240 °C is much higher than those of the reduced catalysts at higher reduction temperatures. The reason is the working catalyst loss into the heavy waxy products due to its poor resistance. The working catalyst loss (measured according to the content of iron in the heavy waxy products) is shown in Fig. 7. The content of the catalysts in the heavy waxy products clearly decreases with the increase

Table 5
Effects of reduction temperature on catalyst activity, stability and product selectivity

	Run no.														
	T240			T250			T260			T270			T280		
	264[a]	407[a]	473[a]	264[a]	430[a]	501[a]	259[a]	474[a]	521[a]	258[a]	429[a]	498[a]	305[a]	449[a]	501[a]
Conversion (mol%)															
CO	60.65	43.75	37.67	64.20	60.06	55.45	64.59	57.60	59.45	63.2	55.79	54.29	55.26	52.53	51.70
H_2	52.97	40.82	35.97	57.29	53.77	50.28	57.11	51.83	53.95	55.5	50.83	49.00	49.25	47.19	46.59
$CO + H_2$	57.58	42.58	36.99	61.44	57.55	53.38	61.60	55.29	57.25	60.1	53.81	49.21	52.85	50.39	49.66
H_2/CO in tail gas (mol/mol)	0.80	0.70	0.68	0.80	0.77	0.74	0.81	0.76	0.76	0.8	0.74	0.74	0.76	0.74	0.74
H_2/CO usage (mol/mol)	0.58	0.62	0.64	0.59	0.60	0.60	0.59	0.60	0.60	0.6	0.61	0.60	0.59	0.60	0.60
Water-gas-shift reaction															
$P_{CO_2} P_{H_2} / P_{CO} P_{H_2O}$	10.70	6.94	5.01	12.16	11.05	9.27	16.12	12.65	14.33	34.5	18.39	20.04	44.82	54.35	46.70
CO_2 selectivity (mol%) (C basis)	46.90	45.03	44.09	46.04	47.58	45.29	48.35	48.03	48.28	47.98	48.49	49.20	49.11	49.20	48.99
Selectivity (wt%) (based on total HC product)															
C_1	2.17	2.04	1.72	2.04	2.13	2.09	2.80	2.92	2.69	3.61	3.67	3.65	4.58	4.58	4.50
$C_{2-4}^{=}$	7.18	7.04	6.10	6.92	7.21	7.13	9.06	9.34	8.50	11.03	11.25	11.11	13.26	13.20	13.06
C_{2-4}	8.59	8.46	7.31	8.34	8.69	8.58	10.98	11.33	10.34	14.20	14.37	14.20	17.13	17.19	17.11
$C_{5-11}^{=}$	8.44	7.15	7.45	8.09	7.73	7.22	9.86	9.74	10.40	11.91	13.76	12.34	14.88	14.30	15.04
C_{5-11}	10.76	9.17	9.74	10.66	10.14	9.84	12.90	12.89	13.65	16.16	18.36	16.42	20.08	19.48	20.46
$C_{12-18}^{=}$	7.23	8.80	10.74	7.24	6.80	8.67	8.13	7.50	7.92	10.03	7.74	7.93	9.89	9.87	9.91
C_{12-18}	13.94	16.70	17.22	13.21	12.86	14.74	14.67	13.03	13.58	16.67	13.78	14.23	17.74	17.47	16.82
C_{19}^{+}	64.54	63.63	64.02	65.74	66.17	64.74	58.65	59.83	59.74	49.36	49.81	51.50	40.46	41.27	41.11
Oxygenates in total HC and oxygenates (wt%)	4.83	3.76	4.29	4.80	4.58	4.28	4.62	5.55	5.03	5.48	6.75	7.16	11.00	10.72	4.28
Oxygenates in water (wt%)	10.37	9.28	9.46	11.45	11.18	10.82	12.77	11.98	11.51	15.77	14.41	15.06	19.85	22.60	24.05
Oxygenates in oil (wt%)	22.39	23.00	22.25	24.03	23.86	24.47	19.41	23.97	22.11	19.21	24.25	26.31	27.05	27.34	25.67

Reaction conditions: 250 °C, 1.5 MPa, H_2/CO = 0.67, 2.0 NL/g-cat h.
[a] TOS (h).

in the reduction temperature. The results clearly indicate that the iron catalyst should be reduced at higher reduction temperatures in order to obtain high activity and favorable stability.

3.4. Product selectivity

The effect of reduction temperature on the product distributions is shown in Table 5 and Fig. 8. Hydrocarbon products are lumped into five groups: C_1 (methane), C_2–C_4 (light hydrocarbon), C_5–C_{11} (gasoline fraction), C_{12}–C_{18} (diesel fraction) and C_{19}^+ (wax). The product distributions display considerable differences at different reduction temperatures. The hydrocarbon distributions shift towards the lower molecular weight of products with the increase in the reduction temperature. The hydrocarbon product selectivities of each test hardly change with time on stream. The catalyst of test T240 has the lowest methane selectivity (~2.0 wt%) and the highest C_{19}^+ selectivity (~64.0 wt%). The catalyst of test T280 has the highest methane selectivity (~4.6 wt%) and the lowest C_{19}^+ selectivity (~41.0 wt%).

It is found that the initial activities and the chain growth probabilities decrease with the increase in the reduction temper-

Table 6
Deactivation rate of the catalyst under different reduction temperatures

Run No.	T240	T250	T260	T270	T280
Deactivation rate (%/d)	2.57	1.08	0.38	0.33	0.33

Reaction conditions: 250 °C, 1.5 MPa, H_2/CO = 0.67, 2.0 NL/g-cat h.

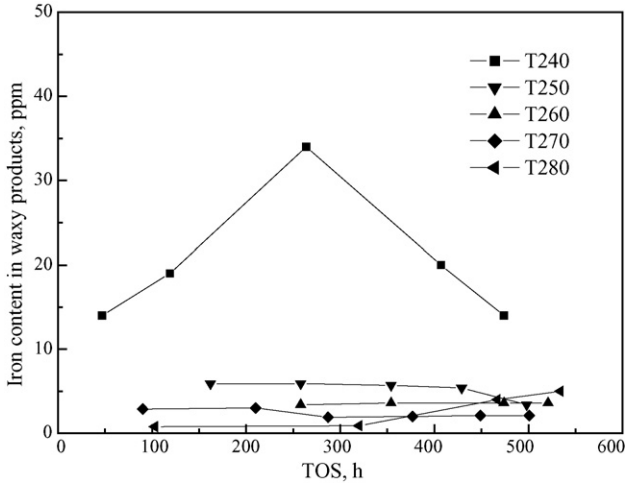

Fig. 7. Effect of reduction temperature on the catalyst loss. Reaction conditions: 250 °C, 1.5 MPa, H_2/CO = 0.67, 2.0 NL/g-cat h.

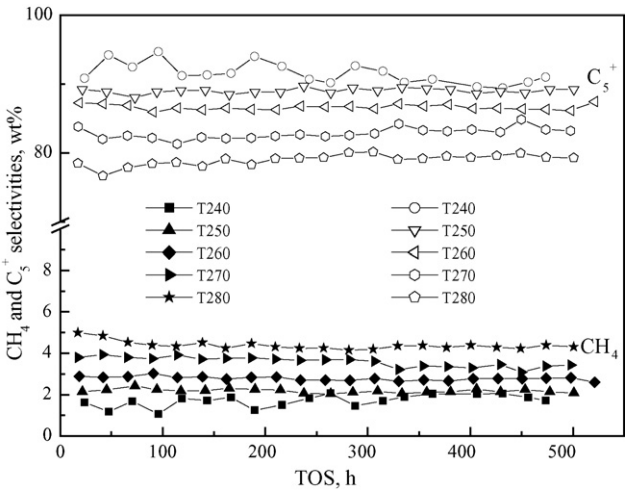

Fig. 8. Effect of reduction temperature on catalyst selectivity. Reaction conditions: 250 °C, 1.5 MPa, $H_2/CO = 0.67$, 2.0 NL/g-cat h.

ature. The carburization is enhanced with increasing reduction temperature and further takes place during the FTS reaction. Some free carbon may be formed during carburization. The deposited free carbon might partition the catalyst surface into some "islands", restricting the diffusion of the monomer for chain growth. Therefore, the increase in deposited carbon with the increase in reduction temperature might result in the decline of the selectivity for heavier products. The other possible reason is that the pore size of reduced catalyst increases with increasing reduction temperature. Large pores facilitate the diffusion of FTS products and may contribute to the formation of much lower molecular weight products.

4. Conclusions

The Fischer–Tropsch reaction over a spray-dried iron-based catalyst reduced at different temperatures was investigated in a 1 dm^3 stirred tank slurry reactor. The effects of reduction temperature on the FTS performance as well as bulk compositions and other properties of the catalyst were studied. The textural properties and phase transformation in the catalyst pretreated at different activation temperatures using syngas play an important role in determining the activity, stability and selectivity of the catalyst. The catalyst particles undergo agglomeration during the pretreatment. The BET surface area and pore volume of reduced catalysts decreases with the increase in the reduction temperature, and the contrary trend is found for pore size.

The content of carbides in reduced catalysts increases with the increase in the reduction temperature. Pretreatment with syngas at higher temperature improves the catalyst activation. The rapid carburization at high reduction temperature results in the formation of a Fe^{3+} (spm) core and an iron carbide layer of the reduced catalyst. On the other hand, the amount of CO_2 released during activation might results in a higher Fe^{3+} (spm) content in the reduced catalyst due to oxidation.

The formation of iron carbides was necessary for obtaining stable high FTS activity. The catalyst activity decreases with the increase in the reduction temperature. The deactivation rate markedly decreases with increasing reduction temperature due to the content of the working catalyst loss in the heavier waxy products.

CH_4 selectivity markedly increases, and the product distributions shift towards lower molecular weight hydrocarbons when the catalyst is reduced at higher temperatures. The increase in deposited carbon at higher reduction temperatures may be responsible for the lower molecular weight of hydrocarbon selectivity.

Acknowledgements

We thank National High Technology Development Program of China, Key Engineering Project of Chinese Academy of Sciences, the National Natural Science Foundation of China for financial support under the contact numbers 2001AA523010, KGC X1-SW-02 and 20590361, respectively.

References

[1] D.B. Bukur, X. Lang, Y. Ding, Appl. Catal. A 186 (1999) 255.
[2] K.R.P.M. Rao, F.E. Huggins, G.P. Huffman, R.J. Gormley, R.J. O'Brien, B.H. Davis, Energy Fuel 10 (1996) 546.
[3] R.J. O'Brien, L. Xu, R.L. Spicer, B.H. Davis, Energy Fuels 10 (1996) 921.
[4] W. van Dijk, H.S. van der Baan, J. Catal. 78 (1982) 24–33.
[5] C.S. Huang, B. Ganguly, G.P. Huffman, F.E. Huggins, B.H. Davis, Fuel Sci. Technol. Int. 11 (1993) 1313.
[6] D.B. Bukur, M. Koranne, X. Lang, K.R.P.M. Rao, G.P. Huffman, Appl. Catal. A 126 (1995) 85.
[7] M.D. Shroff, D.S. Kalakkad, K.E. Coulter, S.D. Köhler, M.S. Harrington, N.B. Jackson, A.G. Sault, A.K. Datye, J. Catal. 156 (1995) 185.
[8] D.B. Bukur, L. Nowicki, R.K. Manne, X. Lang, J. Catal. 155 (1995) 366.
[9] H. Kölbel, M. Ralek, Catal. Rev. Sci. Eng. 21 (1980) 225.
[10] M. Luo, B.H. Davis, Fuel Process. Technol. 83 (2003) 49.
[11] L. Bai, H.W. Xiang, Y.W. Li, Y.Z. Han, B. Zhong, Fuel 81 (2002) 1578.
[12] D.B. Bukur, K. Okabe, M.P. Rosynek, C. Li, D. Wang, K.R.P.M. Rao, G.P. Huffman, J. Catal. 155 (1995) 353.
[13] J.P. Baltrus, J.R. Diehl, M.A. Mcdonald, M.F. Zarochak, Appl. Catal. 48 (1989) 199.
[14] G.B. Raupp, W.N. Delgass, J. Catal. 58 (1979) 337.
[15] C.H. Zhang, Y. Yang, B.T. Teng, T.Z. Li, H.Y. Zheng, H.W. Xiang, Y.W. Li, J. Catal. 237 (2006) 405.
[16] W. Kündig, H. Bommel, G. Constabaris, R.H. Lindquist, Phys. Rev 142 (1966) 327.
[17] B.H. Davis, Department on Energy Final Report, Contract No. DE-FC26-98FT40308, 2002.
[18] N. Sirimanothan, H.H. Hamdeh, Y. Zhang, B.H. Davis, Catal. Lett. 82 (2002) 181.